

# Overview of the NASA Entry, Descent and Landing Systems Analysis Study

Thomas A. Zang<sup>1</sup> and Alicia M. Dwyer-Cianciolo<sup>2</sup>  
*NASA Langley Research Center, Hampton, VA 23681*

David J. Kinney<sup>3</sup> and Austin R. Howard<sup>4</sup> (ELORET)  
*NASA Ames Research Center, Moffett Field, CA 94035*

George T. Chen<sup>5</sup> and Mark C. Ivanov<sup>6</sup>  
*NASA Jet Propulsion Laboratory, Pasadena, CA 91109*

and

Ronald R. Sostaric<sup>7</sup> and Carlos H. Westhelle<sup>8</sup>  
*NASA Johnson Space Center, Houston, TX 77058*

**NASA senior management commissioned the Entry, Descent and Landing Systems Analysis (EDL-SA) Study in 2008 to identify and roadmap the Entry, Descent and Landing (EDL) technology investments that the agency needed to make in order to successfully land large payloads at Mars for both robotic and human-scale missions. This paper summarizes the approach and top-level results from Year 1 of the Study, which focused on landing 10–50 mt on Mars, but also included a trade study of the best advanced parachute design for increasing the landed payloads within the EDL architecture of the Mars Science Laboratory (MSL) mission.**

## I. Introduction

The EDL-SA Study focused on Exploration-class missions in FY 09, i.e., cargo or crewed missions requiring between 10 and 50 mt of landed payload. Candidate technology areas were assessed against a set of eight *EDL-SA Architectures*, i.e., representative architectures (high-level designs) against which the benefits of the technology areas were evaluated. The Study used Design Reference Missions (DRMs), Ground Rules & Assumptions (GR&As) and Figures of Merit (FOMs) that were approved by the managers of the relevant NASA technology programs in May 2009, prior to the execution of the simulations and the evaluations of the FOMs. In evaluating the FOMs, the Study used simulation-based results whenever possible and subjective assessments otherwise. The major simulation-based result was the Mars Arrival Mass, i.e., the total mass of the payload plus the systems needed for Mars Orbit Insertion and Mars EDL. A comprehensive report of the EDL-SA Study is given in Ref. [i]. Specialized aspects of the Study are discussed in detail in Refs. [ii, iii, iv, v, vi, vii, viii, ix, x].

## II. Exploration-class Technologies and Architectures

The EDL-SA Team held a brainstorming session in November 2008 to identify candidate technologies for consideration. The context for the technology brainstorming was the Exploration-class DRM, namely, the

---

<sup>1</sup> Chief Technologist, Systems Analysis and Concepts Directorate, MS 449, AIAA Associate Fellow

<sup>2</sup> Aerospace Engineer, Atmospheric Flight and Entry Systems Branch, MS 489, AIAA Senior Member

<sup>3</sup> Aerospace Engineer, Systems Analysis & Integration Branch, MS 258-1

<sup>4</sup> Aerospace Engineer, ELORET Corp, Systems Analysis & Integration Branch, MS 258-1, AIAA Member

<sup>5</sup> Group Supervisor, Entry, Descent, and Landing Systems & Advanced Technologies Group, MS 313H

<sup>6</sup> Mission Design Engineer, Entry, Descent, and Landing Systems & Advanced Technologies Group, MS 343B

<sup>7</sup> Aerospace Engineer, Flight Mechanics and Trajectory Design Branch, MS EG5, AIAA Senior Member

<sup>8</sup> Aerospace Engineer, Flight Mechanics and Trajectory Design Branch, MS EG5

aerocapture and EDL phases of the Mars Design Reference Architecture 5.0 [xi] (DRA5). One of the Ground Rules for the Study was that the only changes permitted to DRA5 were in the aerocapture and EDL phases. (The Design Reference Missions, the Ground Rules and Assumptions and the Figures of Merit for the FY 09 EDL-SA Study are given in Ref. [i].) The baseline EDL architecture—Architecture 1—was that of DRA5: a rigid, mid-L/D aeroshell used for aerocapture and hypersonic entry deceleration, followed by supersonic retro-propulsion for descent and ending with subsonic retro-propulsion through landing. Alternatives to this concept were then identified using a common “tree” approach, and refined by engineering judgment and the availability of reasonable models.

The technology areas that emerged from this brainstorming and subsequent refinement were

- Rigid Mid-L/D Aeroshells (Rigid Mid-L/D AS)
- Hypersonic Inflatable Aerodynamic Decelerators (HIAD)
- Supersonic Retro-Propulsion (SRP)
- Supersonic Inflatable Aerodynamic Decelerators (SIAD)
- Deployable Supersonic IADs With Skirt (SIAD–Skirt)
- Dual-Pulse Thermal Protection Systems (DP Flexible TPS and DP Rigid TSP)

One example of a Rigid Mid-L/D Aeroshell is the *ellipsled* used in DRA5. For Inflatable Aerodynamic Decelerators (IADs), the main distinctions are whether the IAD operates in the hypersonic regime (H) or the supersonic regime (S) and whether it primarily provides lift (L) or drag (D). For the thermal protection systems, there is an important distinction between TPS for flexible aeroshells (for IADs) or for rigid aeroshells.

During the initial screening process, methods of hard landing such as airbags were eliminated, so all of the architectures assumed powered subsonic phases as the only practical way to attain pinpoint landings next to pre-deployed assets, as required by DRA5. Engineering details such as leg design, crushable segments, and stroke length were not studied. A hazard detection and avoidance system is considered necessary, but sensor requirements were not evaluated in the Year 1 activities.

For the purposes of performance simulations, and to stay within the constraints of the Study schedule and budget, simplifications were made for modeling the various technologies. The important parameters of aerodynamic decelerators at this level are frontal area, aerodynamic characteristics, and mass. For instance, a HIAD was assumed to have enough internal pressure to act as a rigid blunt body. All propulsion stages, whether in the hypersonic, supersonic or subsonic regimes, used a common mass and sizing model.

In keeping with standard practice in systems analysis for technology evaluation, the technologies were assessed against the suite of EDL-SA Architectures. The set of EDL-SA Architectures only needs to include options that encompass all candidate technology areas. The architecture suite is illustrated in Figure 1, and the resulting simplified set of technologies is listed in Table 1. Evaluation of the technologies is accomplished by evaluating metrics at the architecture level, and then extracting the benefits (or penalties) of the technologies pairwise by comparison of architectures that differ only in the specific technologies.

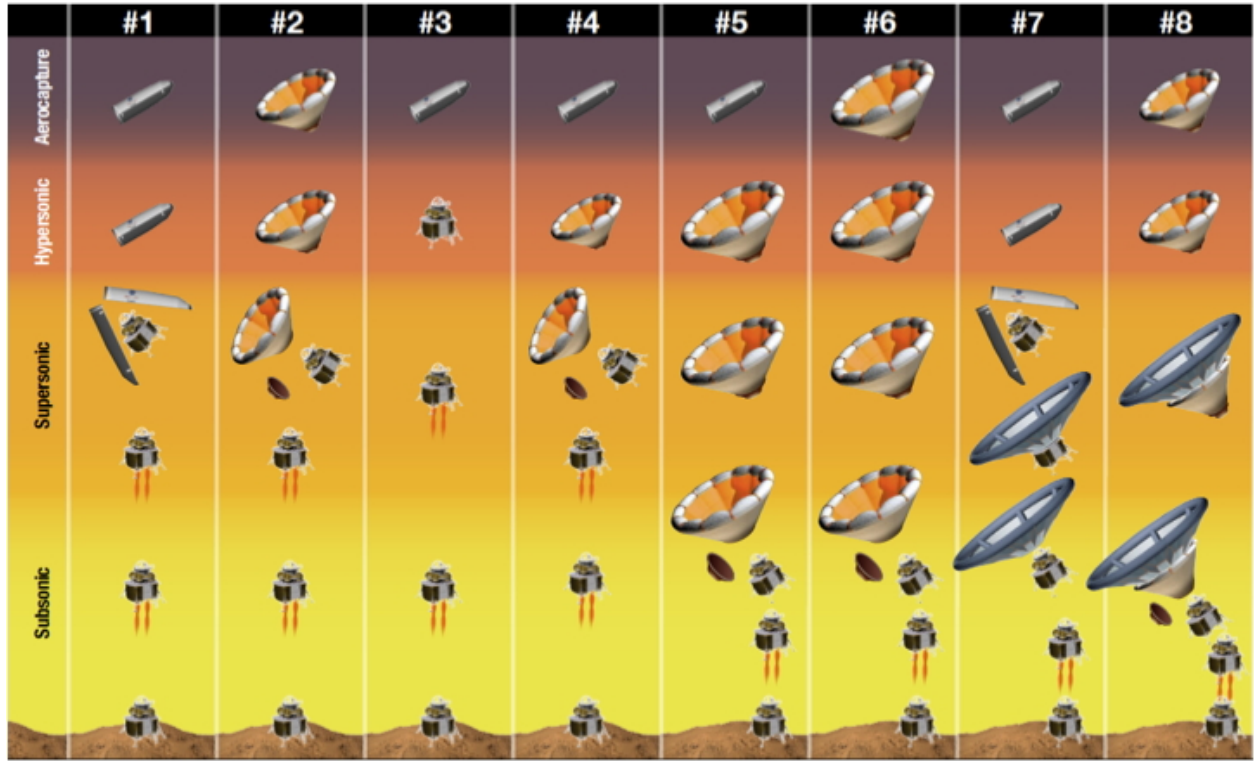


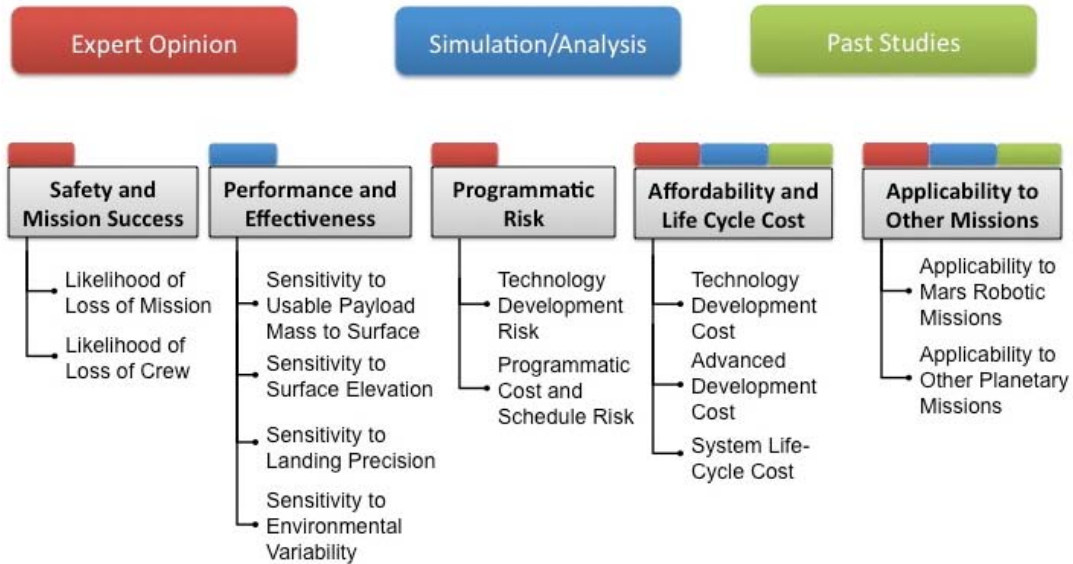
Figure 1. Exploration-class Architectures

Table 1. Simplified Set of Exploration-Class Technologies Considered by EDL-SA

	Aerocapture	Hypersonic	Supersonic	Subsonic
Architecture 1	Rigid Mid-L/D AS	Rigid Mid-L/D AS	Propulsion	Propulsion
Architecture 2	Lifting HIAD	Lifting HIAD	Propulsion	Propulsion
Architecture 3	N/A	Propulsion	Propulsion	Propulsion
Architecture 4	Rigid Mid-L/D AS	Lifting HIAD	Propulsion	Propulsion
Architecture 5	Rigid Mid-L/D AS	Lifting HIAD	Same LHIAD	Propulsion
Architecture 6	Lifting HIAD	Lifting HIAD	Same LHIAD	Propulsion
Architecture 7	Rigid Mid-L/D AS	Rigid Mid-L/D AS	Drag SIAD	Propulsion
Architecture 8	Lifting HIAD	Lifting HIAD	LSIAD-Skirt	Propulsion

### III. Figures of Merit

The architecture and technology assessment was performed in terms of their impact upon the Figures of Merit (FOMs) illustrated in Figure 2. There are thirteen individual FOMs spread across five categories. The sources of data upon which the FOMs were evaluated included results from the simulations and analyses of the EDL-SA Team, from results of past studies and from expert opinion. The figure indicates the sources used in each FOM category. In most cases the FOMs were evaluated from proxy parameters, which can discriminate between the architectures and technologies. For example Arrival Mass is one of the proxy parameters for System Life-Cycle Cost; Technology Readiness Level (TRL) and R&D Degree of Difficulty (RD3) are proxy parameters for Technology Development Risk and Technology Development Cost. The FOMs and their proxy parameters were reviewed and approved (with some modifications) by the relevant technology program managers in May 2009.



**Figure 2. Figures of Merit for Exploration-class Architectures & Technologies**

Detailed descriptions of the processes used to evaluate the Figures of Merit and the results for the FOMs are presented in a companion paper in this conference (Ref. [ii]) as well as in Ref. [i].

#### IV. Component Models

The principle component models used in the study were for mass, aerodynamics and aerothermodynamics, flight mechanics, guidance, retro-propulsion and thermal protection systems.

The EDL-SA architecture suite contains five unique components (see Figure 1 and Figure 3): rigid mid-L/D aeroshell, lifting hypersonic inflatable decelerator (LHIAD), drag supersonic inflatable decelerator (DSIAD), lifting supersonic inflatable decelerator implemented with a skirt on an LHIAD (LSAID-Skirt), and retro-propulsion (RP). Parametric mass models were developed for each these five components. Details are provided in Ref. [vii] (a summary is given in Ref. [i]). An example of the mass breakdown for Architecture 1 is given in

Table 2.

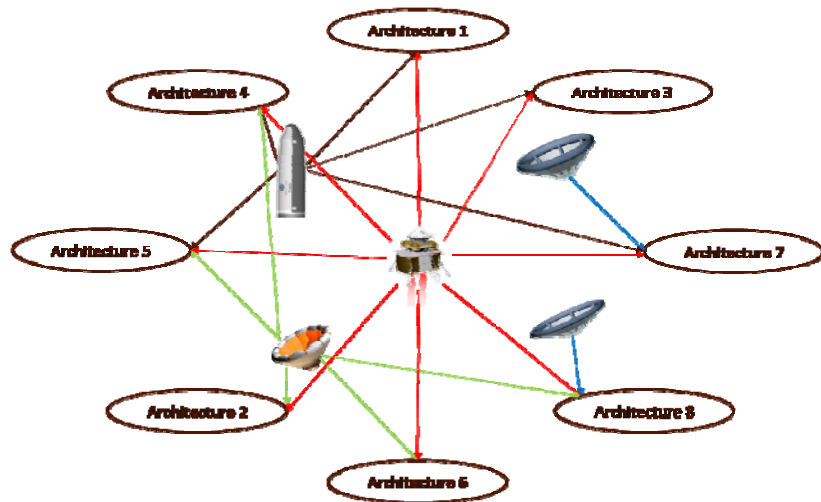


Figure 3. Major Mass Components

**Table 2. Nominal Parameters and Mass Breakdown for Architecture 1**

Variable	Value	Mass Components	kg
Diameter, m	10	Structure	5482
Length, m	30	Acoustic Blanket	6415
Aerocapture Heat Load, MJ/m <sup>2</sup>	345	Separation System	2065
Entry Heat Load, MJ/m <sup>2</sup>	130	Avionics	222
Max Dynamic Pressure, kPa	11	Flap	1729
Max Lateral Deceleration, m/s <sup>2</sup>	29	TPS	9199
Max Axial Deceleration, m/s <sup>2</sup>	4	Total	25112
Arrival Mass, mt	110		

The aerodynamic and aerothermal models cover Mach 1.3 through 50, angles of attack of 0 through 90 deg, and dynamic pressures of  $10^{-7}$  through 0.75 bars. The aerodynamic models cover body flap deflections in the range of -10 to 50 deg, and a speed brake for the range of 0 to 60 deg. The aerodynamic model was developed by blending results from three separate levels of fidelity—linear (CBAERO), Euler (CART3D) and Reynolds-averaged Navier-Stokes (DPLR). Details are provided in Ref. [viii] (a summary is given in Ref. [i]).

In the flight mechanics component the approach velocities and target orbits for the cargo and crewed vehicles were provided by DRA5. To summarize: 1) the hyperbolic approach velocity was set at 7.36 km/s; 2) the target orbit was 1 Sol (33793 km x 250 km); 3) EDL initiates from the 1 Sol orbit; 4) the landing site is at 0 km altitude; 5) the touchdown provides 10 m accuracy; and 6) the deceleration profiles remain within those limits set for a deconditioned crew (Ref. [xii]) (while allowing for dispersions). It was assumed for all the architectures that a reaction control system (RCS) would be the primary control. To emulate the characteristics of a RCS without having to design a control system, a *pseudo-controller* that modeled the bank acceleration, maximum bank rate, and bank direction was used. The aerocapture evaluation used the HYPAS (Hybrid Predictor-Corrector Aerocapture Scheme) guidance algorithm to provide bank angle commands.

Evaluations for the Monte Carlo performance analyses and the sensitivity analyses were done using the *theoretical guidance* algorithm. The performance analysis and the sensitivity analysis are described in detail in Ref. [iii] and Ref. [iv], respectively (a summary is given in Ref. [i]). The theoretical guidance is representative of the functionality of a guidance algorithm, but has full knowledge of all environmental parameters (aerodynamics, atmosphere, etc.) The Analytic Predictor-Corrector guidance used in the Study is a combination of a modified Apollo entry guidance and the Apollo powered-descent guidance. The Numerical Predictor-Corrector guidance integrates a simplified set of the equations of motion and iterates the appropriate control parameter to meet the specified constraints. The guidance algorithms are described in detail in Ref. [v] (a summary is given in Ref. [i]).

The sizing analysis for the thermal protection system (TPS) is based on the tools and practices developed by the Orion TPS Advanced Development Project. The TPS sizing tool was extended for EDL-SA to include the capability to size dual-layer TPS. The TPS analyses are described in detail in Refs. [ix] and [x] (a summary is given in Ref. [i]).

## V. Simulations

The simulation used to evaluate the EDL-SA architectures is the Program to Optimize Simulated Trajectories (POST2), which has extensive heritage for simulating ascent, descent, and orbiting trajectories. The code employs standard atmosphere, planet and gravity models as well as EDL-SA specific models described in previous sections including aerodynamic and aerothermodynamics, mass properties, guidance, propulsion and terminal descent. Navigation is assumed to be perfect throughout the trajectory. Details of the simulations used for the aerocapture and EDL phases are provided in Ref. [vi] and Ref. [iii], respectively. In this paper we provide a summary of the simulation results.

Table 3 summarizes the IAD sizes and the system ballistic numbers, and Table 4 furnishes the component mass breakdown for all eight architectures. The Arrival Mass is highlighted because it is a key proxy variable for the Life-Cycle Cost FOM. High-level summaries of the optimized trajectories for each architecture are provided in the remainder of this section. Considerably more details, including the Monte Carlo results, are available in Refs. [i] and [iii].

**Table 3. IAD Diameters and System Ballistic Numbers**

<b>Architecture</b>	<b>1</b>	<b>2</b>	<b>3</b>	<b>4</b>	<b>5</b>	<b>6</b>	<b>7</b>	<b>8</b>
HIAD Diameter (m)	--	23.0	--	23.0	67.8	81.9	--	23.0
Aerocapture/Entry SIAD Diameter (m)	--	--	--	--	--	--	44.6	44.3
Aerocapture/Entry BN (kg/m <sup>2</sup> )	396.1	154.0	--	134.6	20.6	20.4	412.0	152.5
Descent BN (kg/m <sup>2</sup> )	--	--	--	--	--	--	27.2	40.8

**Table 4. Component Mass Breakdown**

<b>Architecture</b>	<b>1</b>	<b>2</b>	<b>3</b>	<b>4</b>	<b>5</b>	<b>6</b>	<b>7</b>	<b>8</b>
<b>Arrival Mass</b>	<b>110.1</b>	<b>83.6</b>	<b>265.2</b>	<b>109.0</b>	<b>133.5</b>	<b>140.5</b>	<b>107.4</b>	<b>80.6</b>
Deorbit Mass	109.2	82.8	188.1	75.1	98.0	139.4	106.3	79.6
Aeroshell, AS (Total)	28.9	0.0	--	26.0	27.0	0.0	28.8	0.0
AS Structure	18.3	--	--	18.4	19.3	--	18.2	--
AS TPS	10.6	--	--	7.6	7.6	--	10.6	--
Avionics and Separation Structure	2.0	2.1	--	4.3	7.4	8.5	2.0	1.9
Entry RCS (Total)	10.8	7.1	--	9.9	14.7	16.8	11.7	7.4
RCS Dry Mass	5.2	2.7	--	5.8	9.2	9.9	6.1	2.9
RCS Propellant	5.5	4.4	--	4.1	5.5	6.9	5.6	4.5
HIAD (Total)	--	10.6	--	6.0	25.7	56.0	--	10.6
HIAD Structure	--	6.0	--	3.1	10.7	22.3	--	5.9
HIAD TPS	--	4.7	--	2.9	15.0	33.7	--	4.7
SIAD Mass	--	--	--	--	--	--	6.8	2.1
Descent Stage, DS	28.4	23.8	148.1	22.8	18.7	19.2	18.1	18.6
DS Dry Mass	12.3	11.7	19.2	11.2	9.9	10.5	10.2	10.4
DS Propellant	16.2	12.0	128.9	11.6	8.8	8.7	7.9	8.2
Landed Mass	52.3	51.8	74.7	51.2	49.9	50.5	50.2	50.4
Payload Mass	40.0	40.0	40.0	40.0	40.0	40.0	40.0	40.0

### *Architecture 1*

The Architecture 1 entry configuration, selected for its similarity to DRA5, includes a rigid mid-L/D aeroshell for aerocapture and hypersonic flight along with retro-propulsion for descent and landing. Figure 4 (left) shows the timeline below 30 km. The vehicle flies at 55 deg angle of attack and has a L/D of 0.5. The Arrival Mass estimate for DRA5 of 110 mt and the higher fidelity EDL-SA Arrival Mass of 110.1 mt reported in Table 3 are essentially identical, implying that the approximations made for DRA5 adequately represent current knowledge.

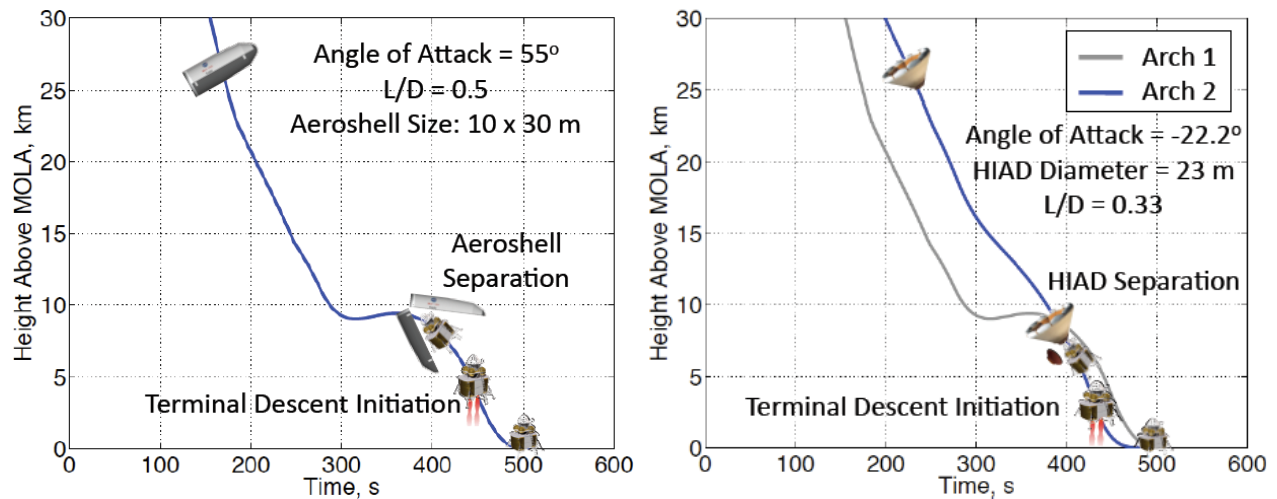


**Figure 4. Architectures 1 (left) and 2 (right) Nominal Altitude vs. Time**

### *Architecture 2*

Architecture 2, which uses a LHIAD for aerocapture and entry along with supersonic retro-propulsion, was selected to evaluate the mass savings of using a HIAD with dual-pulse flexible TPS over a rigid mid-L/D aeroshell with dual-pulse rigid TPS. The 23 m inflatable design is based on the MIAS concept (Ref. [xiii]) and is currently at a lower TRL than the rigid mid-L/D aeroshell. The angle of attack for the vehicle is -22 deg, and the L/D is 0.33. Figure 4 (right) provides its timeline along with the timeline curve for Architecture 1. For Architecture 2 the range-to-target at terminal descent initiation has been reduced from that of Architecture 1 (from 11 km to 5 km), resulting in reduced timeline margin for terminal descent. However, use of the LHIAD, based on the mass models developed for EDL-SA, reduces the Arrival Mass over Architecture 1 by more than 26 mt.

### *Architecture 3*

Architecture 3, the all-propulsive entry configuration, was the least complex EDL alternative and, using only engines, was considered relatively high TRL compared to the other architectures. The analysis used for this architecture differed from that used for all the others. In particular, POST2 is used to compute the required  $\Delta V$ , assuming that the engines burn continuously from the engine initiation point; the sizing tool iteratively computes (and optimizes) many parameters, including propellant and structural component masses, inert mass fraction and engine initiation altitude, and it utilizes the EXAMINE mass model Ref. [xiv]. (With the rocket plume surrounding the vehicle upon entry through the atmosphere, the analysis assumes that the drag was zero, which may be conservative, and that the surface aerodynamic heating does not require additional TPS, which may be optimistic. Moreover, the mass required to put the system in the 1 Sol orbit upon arrival is not accounted for.) The minimal Arrival Mass was 265 mt using LOX/LCH4 engines. This configuration had the largest Mars Arrival Mass, several times larger than any other considered for EDL-SA.

### *Architecture 4*

The entry portion of Architecture 4 is identical to Architecture 2. However, consideration was given to Architecture 4 to compare the mass savings of using a single use (entry only) TPS on a 23 m HIAD to the dual use (aerocapture and entry) version used in Architecture 2. Therefore, in contrast to Architecture 2, Architecture 4 uses a rigid aeroshell for aerocapture, then, prior to entry, the HIAD is inflated. The result is a larger Arrival Mass of 109 mt compared to Architecture 2's 83.6 mt, but the entry mass is lighter by almost 8 mt due, in part, to the 4 mt lighter HIAD mass. The timeline is provided in Figure 5 (left). The component mass numbers are compared in Table 3. The added launch mass, the development and increase in mission complexity of using a separate aerocapture system, as well as the technical challenges already present in Architecture 2 make this configuration unattractive.



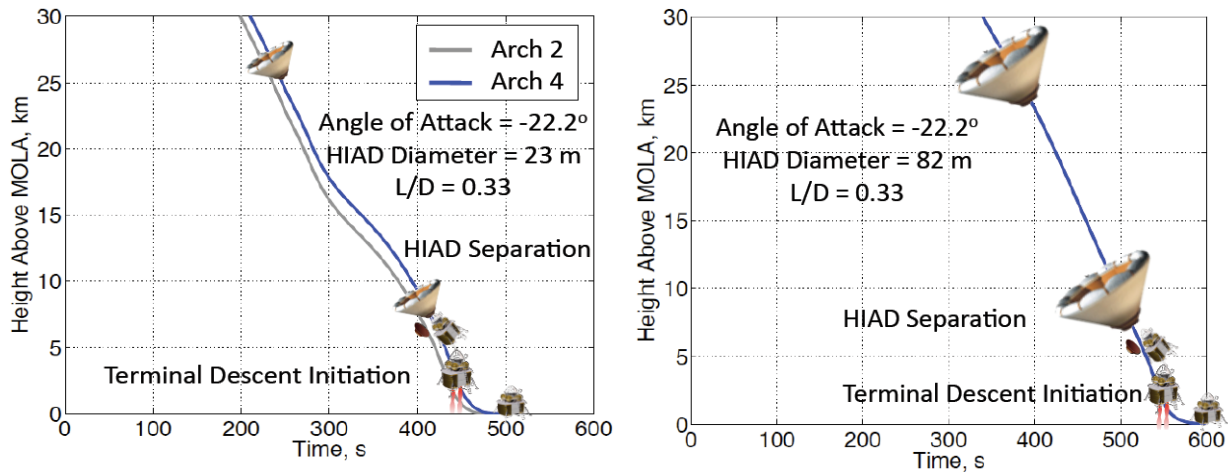


**Figure 5. Architectures 4 (left) and 6 (right) Nominal Altitude vs. Time**

### *Architectures 5 and 6*

Architectures 5 and 6 were selected to compare the mass savings of using a very large HIAD to subsonic speeds in the event that supersonic retro-propulsion, considered in Architectures 2 and 4, proves to be an unusable option for an Exploration-class mission. Architecture 5, like Architecture 4, compared the mass saving of using a single use TPS HIAD for entry and a rigid aeroshell for aerocapture. The simulation optimized the HIAD diameters to be 68 m and 82 m for Architectures 5 and 6, respectively. While the mass of the aeroshell and smaller HIAD in Architecture 5 did result in a lower Arrival Mass than Architecture 6’s dual use HIAD, there was an issue in the mass model used for both architectures that calls all the results into question. The issue is that the TPS mass model used for the large HIADs was limited to a 50 m diameter. Extrapolation beyond that diameter resulted in the assumption that the areal density of the material was constant, which is not likely to be the case. Also there are additional EDL timeline challenges of successfully slowing the vehicle to subsonic speeds with adequate altitude margin to initiate the terminal descent engines and land at the target. The time line for Architecture 6 is provided in Figure 5 (right); Architecture 5 is very similar. A low throttle setting of nominally 65% is used to slow the vehicle starting at approximately 2.5 km such the at vehicle can touch down at the target. The large diameter HIAD flies at the same angle of attack -22 deg and same L/D as in Architecture 2. The results indicate that investments in supersonic retro-propulsion might be a more prudent over 70 m HIAD systems, which have packaging and separation technical challenges.

### *Architecture 7*

In the same spirit, Architecture 7 was selected as an alternative to Architecture 1 assuming that supersonic retro-propulsion was an infeasible option for Exploration-class missions. Architecture 7 replaces supersonic retro-propulsion with a 51 m diameter SIAD and subsonic retro-propulsion. The nominal time line compared to Architecture 1 is shown in Figure 6 (left). The entry strategy remains the same. To accommodate wind effects on the large unguided SIAD, a cross range offset at entry was included in the simulation. The altitude at engine initiation was also maximized to account for the winds and unguided portion of the trajectory. Therefore, the maximum throttle setting during terminal decent was reduced from 80 to 65%, as well as the system thrust-to-weight from 3.0 to 2.5 g’s. In addition to the aeroshell packaging and separation technical challenges, Architecture 7 has SIAD packaging, deployment, inflation and separation technical challenges. In the end, the added complexity of EDL for Architecture 7, in particular the unguided portion of the trajectory on the SIAD, produces a mass savings of only 3 mt of Mars Arrival Mass compared to Architecture 1.

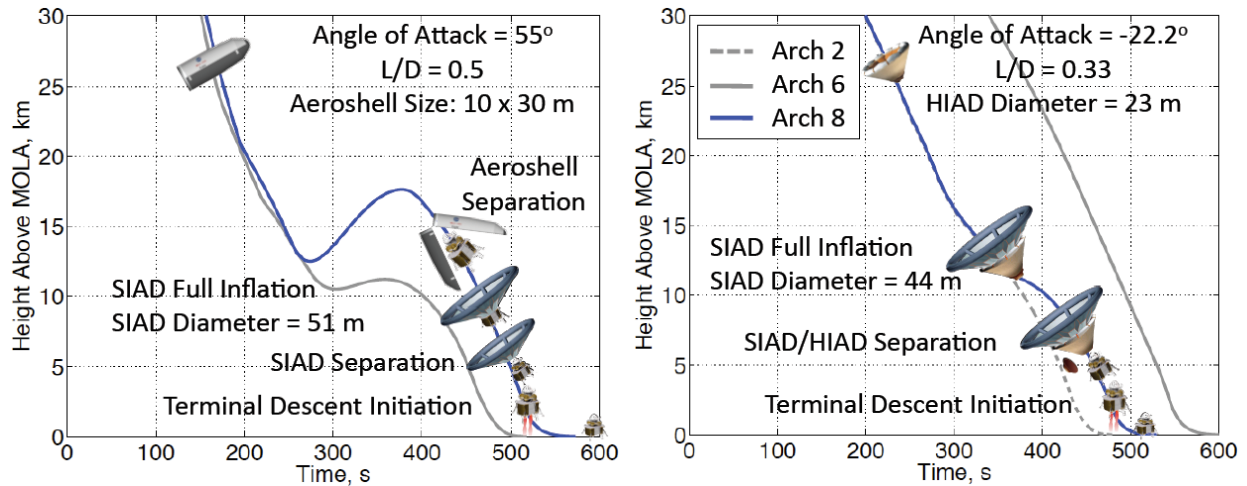


**Figure 6. Architecture 7 (left) and 8 (right) Nominal Altitude vs. Time**

### *Architecture 8*

Architecture 8 considered a LHIAD plus LSIAD configuration as an alternative to a single large LHIAD (Architecture 6) to reduce the vehicle to subsonic speeds prior to engine initiation. The LHIAD/LSIAD combination included the same 23 m LHIAD used in Architectures 2 and 4. See Figure 6 (right) for the timeline. The simulation determined the size of the LSIAD and its nominal deployment—44 m and Mach 2.6, respectively—such that the terminal descent engine initiation would occur at subsonic speeds. Since a LSIAD is deployed after peak heating, a TPS is not needed, and, therefore, there is a mass advantage. The simulation results indicate that Architecture 8 has a 38 mt Arrival Mass advantage over Architecture 6 (see Table 3). And if the use of a LHIAD/LSIAD combination is compared to using supersonic retro-propulsion in Architecture 2, the use of a LSIAD still saves approximately 3 mt.

## **VI. Exploration-class Study Recommendations**

The key enabling technology areas identified for investments from the EDL-SA Study results were rigid aeroshells, deployable/inflatable decelerators, supersonic retro-propulsion, aerocapture, and all-propulsive EDL systems. Although not included in the FY 09 analyses, there is also the need for precision landing with hazard avoidance. The recommended investment roadmap and details on the specific technology areas will be included in the final paper.

The lowest Arrival Mass is associated with use of deployable/inflatable decelerators. Rigid aeroshells offer a more traditional solution, despite a 35% Arrival Mass penalty compared with an inflatable decelerator. Supersonic retro-propulsion reduces the sensitivity to environmental variability compared with supersonic/subsonic aerodynamic decelerators. However, both inflatables and supersonic retro-propulsion need significant development before concerns about their controllability can be allayed. Precision landing requirements have never been demonstrated. Aerocapture is enabling (in the absence of NTR) and has never been demonstrated. The all-propulsive architecture warrants further investigation despite its 200%+ Arrival Mass penalty because of its high ratings on the Safety and Mission Success and Programmatic Risk FOMs. Moreover, significant engineering work will be needed to ensure reliable mechanisms are developed for transitioning between the configurations during EDL.

**Table 5. TDP Recommendations**

<b>Technology Area</b>	<b>TDP Content</b>
Rigid Decelerators	Tools & processes for generating aero/aerothermal databases & mass models; rigid, dual heat-pulse capable TPS; structures; rigid decelerator (aeroshells and deployables) shapes for aerodynamic performance and controllability; vehicle designs
Flexible Decelerators	Tools & processes for generating aero/aerothermal databases & mass models for flexible entry/aerocapture vehicles; flexible materials, flexible decelerator shapes for aerodynamic performance, structural strength and controllability; vehicle designs
Precision Landing	Sensors, navigation and controls and their integration for precision landings with hazard avoidance in atmospheres
Supersonic Retro-Propulsion	Aero-propulsion interaction propulsion for supersonic deceleration—tools, controls, and configurations. Works for high supersonic initiation through touchdown.
All-propulsive Design	System studies of open issues for hypersonic phase and staging
Aerocapture Development	Requirements for an Aerocapture Technology Validation Flight Test
Supersonic Retro-Propulsion Flight Test Program	Flight demonstration (TRL=6) of controllability from initiation to simulated touchdown of supersonic retro-propulsion descent system.
Deployable Decelerator Flight Test Program	Flight demonstration (TRL=6), including controllability of Deployable, Inflatable Aerodynamic Decelerator
Aerocapture Flight Test	Flight demonstration (TRL=6–7) in upper Earth atmosphere
Parachute Flight Test Program	Flight testing of a supersonic Ringsail parachute, including reefing and deployment of a large (>21.5m diameter) parachute at Mach >2.0

**VII. Large-robotic-class Study**

The robotic analysis focused on delivering 1500 kg to 0 km MOLA through the use of enhanced parachute designs on an MSL-type entry vehicle. The parachute type, size, and quantity were varied to achieve the desired payload performance. To mitigate the parachute design modifications from current technology, the MSL entry capsule’s L/D was also increased by flying at a larger angle of attack throughout the entry phase. Single, dual, and reefed parachute strategies were explored as well as two different parachute designs for each strategy: disk gap band (DGB) and ringsail. In addition, a systems engineering analysis was performed to assess the ability of the current 4.5 m MSL aeroshell to adequately package a 1500 kg payload.

A survey of past test flights was performed to determine the aerodynamic modeling for each parachute design. The current MSL parachute is a 21.5 m diameter DGB type design but a ringsail design is known to generally have better subsonic drag performance than a DGB parachute. Although popular for subsonic applications, the ringsail parachute design has had limited supersonic flight test experience, making the determination of its supersonic drag characteristics an especially challenging process due to lack of data. A reefed parachute is simply a single parachute that opens in stages to better guarantee a successful deployment, especially with very large diameter designs. Since it was expected that parachutes far in excess of 21.5 m would be required to land a 1500 kg payload, a reefed chute design option was desirable.

As a consequence of the large 1500 kg payload mass and 0 km landing elevation, it was determined that the packing density resulting from integrating the payload into the MSL 4.5 m aeroshell was exceedingly large. A more favorable approach was to increase the aeroshell diameter to 4.7 m, a value closer to the limit that current launch vehicle fairings will allow. In addition, the number of engines on the MSL descent stage would have to increase from 8 to 12 engines in order to maintain a thrust to weight similar to that of MSL during the powered descent phase. Finally, 300 kg more propellant (700 kg total) was necessary to successfully land the larger payload mass. All these modifications were incorporated into the DRM used in the parachute sizing analysis. The parachute sizing analysis resulted in the solutions summarized in

Table 6.

**Table 6. Parachute Sizing Solutions**

Parachute Configuration	DGB	Ringsail
Single Chute		
Diameter (m)	32.5	31.5
Deploy Mach	2.5	2.5
Dual Chute		
1 <sup>st</sup> /2 <sup>nd</sup> Diameter (m)	21.5/41.5	21.5/41.0
1 <sup>st</sup> /2 <sup>nd</sup> Deploy Mach (3 $\sigma$ high)	2.5/1.5	2.5/1.5
Reefed Chute		
Reefed/Disreefed Diameter (m)	21.5/34.0+	21.5/34.0
Reefed/Disreefed Deploy Mach (3 $\sigma$ high)	2.5/2.0	2.5/2.0

Due to its slightly smaller size requirements and excellent subsonic performance, a reefed ringsail is the recommended parachute solution to landing 1500 kg at 0 km MOLA.

### VIII. Future Work

For FY 10, the focus of EDL-SA shifted to identification of technologies for landing large robotic payloads on Mars. Two related studies are underway. The first is looking at technologies for an EDL system using minimum improvements to Mars Science Laboratory technology to deliver 1.0–1.3 mt of landed mass. The second is looking at an EDL systems capability of landing 2–3 mt, using technologies needed to support the Exploration-class EDL development technologies determined in FY 09.

### IX. Acknowledgments

The members of the EDL-SA Team, coming from four NASA Centers—ARC, JPL, JSC, LaRC—and numbering more than 30, are too numerous to list here individually. The work summarized in this paper is based on all of their contributions, as well as those of the various stakeholders and reviewers of the team’s work. See Ref. [i] for complete lists of team members, stakeholders and reviewers.

### X. References

- 
- <sup>i</sup> Dwyer-Cianciolo, A. M., et al., “Entry, Descent and Landing Systems Analysis Study: Phase 1 Report,” NASA–TM–2010–216720, July 2010.
- <sup>ii</sup> Howard, A., Stanley, D., and Williams-Byrd, J., “Mars Exploration Entry and Descent and Landing Technology Assessment Figures of Merit,” AIAA SPACE 2001 Conference and Exposition, Anaheim, CA, Aug. 30–Sept. 2, 2010.
- <sup>iii</sup> Dwyer-Cianciolo, A. M., Davis, J. L., Shidner, J. D., and Powell, R. W., “Entry, Descent and Landing Systems Analysis: Exploration Class Simulation Overview and Results,” AIAA–2010–7970, 2010.
- <sup>iv</sup> Shidner, J. D., Davis, J. L., Dwyer-Cianciolo, A. M., Powell, R. W., and Samareh, J. A., “Large Mass, Entry, Descent and Landing Sensitivity Results for Environmental, Performance, and Design Parameters,” AIAA–2010–7973, 2010.
- <sup>v</sup> Davis, J. L., A.M. Dwyer-Cianciolo, Powell, R. W., Shidner, J. D., and Llama, E. G., “Guidance and Control Algorithms for the Mars Entry, Descent and Landing Systems Analysis,” AIAA–2010–7972, 2010.
- <sup>vi</sup> Zumwalt, C. H., Sostaric, R. R., and Westhelle, C. H., “Aerocapture Guidance and Performance at Mars for High-Mass Systems,” AIAA–2010–7971, 2010.
- <sup>vii</sup> Samareh, J. A., and Komar, D. R., “Parametric Mass Modeling for Mars Entry, Descent, and Landing System Analysis Study,” abstract submitted to the 49<sup>th</sup> AIAA Aerospace Sciences Meeting, Orlando, FL, January 4–7, 2011.
- <sup>viii</sup> Kinney, D. J., “Aerodynamic and Aerothermal Environment Models for a Mars Entry, Descent, and Landing Systems Analysis Study,” abstract submitted to the 49<sup>th</sup> AIAA Aerospace Sciences Meeting, Orlando, FL, January 4–7, 2011.
- <sup>ix</sup> McGuire, M. K., Arnold, J. O., Covington, M. A., Dupzyk, I. C., “Flexible Ablative Thermal Protection Sizing on Inflatable Aerodynamic Decelerator for Human Mars Entry Descent and Landing,” abstract submitted to the 49<sup>th</sup> AIAA Aerospace Sciences Meeting, Orlando, FL, January 4–7, 2011.

---

<sup>x</sup> McGuire, M. K., “Dual Heat Pulse, Dual Layer Thermal Protection System Sizing Analysis and Trade Studies for Human Mars Entry Descent and Landing,” abstract submitted to the 49th AIAA Aerospace Sciences Meeting, Orlando, FL, January 4–7, 2011.

<sup>xi</sup> Drake, B. G. (ed.), “Human Exploration of Mars Design Reference Architecture 5.0,” NASA-SP-2009-566, July 2009.

<sup>xii</sup> NASA Human-Systems Integration Requirements, CxP 70024, Rev C, Oct.31, 2008.

<sup>xiii</sup> MIAS Design Reference Report, Astrium GmbH, MIAS-RIBPRE-RP-0002, Dec. 4, 2002 (Unpublished).

<sup>xiv</sup> Komar, D. R., Hoffman, J., and Olds, A., “Framework for the Parametric System Modeling of Space Exploration Architectures,” AIAA-2008-7845, 2008.